# A Model-Assisted Probability of Detection (MAPOD) Approach for Enhancing the Reliability of Ultrasonic Inspection in Adhesive Bonded Joints

GAWHER AHMAD BHAT[1,*] and ELENA JASIUNIENE[1,2]

**ABSTRACT**
This study presents a model-assisted technique to investigate the probability of detection (POD) for ultrasonic inspection of adhesive joints with defects (brass inclusions and delamination). Numerical simulations using CIVA software were conducted to predict how ultrasonic waves respond to flaws of varying sizes from 0.01 mm to 5 mm. A sensitivity analysis was performed to simplify the physics-based model by identifying the most influential parameter using a meta-model. The model was further improved and calibrated to generate a POD curve, enabling accurate determination of the smallest detectable crack size. Moreover, this study focused on the implementation of a custom-developed Python script to integrate ultrasonic features (absolute time-of-flight difference, maximum amplitude, and absolute energy) for evaluating the POD curve, while also addressing statistical uncertainties arising from measurement noise, material variability, and discrepancies in simulation models. Confidence intervals were added to reflect uncertainties in the simulation parameters and to predict potential differences between both simulation and real adhesive-bonded structural integrity. The results of this study revealed that the potential of model-assisted probability of detection (MAPOD) analysis enhanced the detection and measurement of defects in adhesive-bonded joints. Overall, these results make a valuable contribution to improving quality control, effective structural health monitoring and advancement in reliable predictive methods for non-destructive testing (NDT).
**Keywords:** Non-destructive testing, model-assisted POD, ultrasonic testing, sensitivity analysis, adhesive bonded joints

## 1. Introduction

Adhesive bonded joints have been widely used in different industries due to their numerous advantages [1-4]. The adhesive bonded joints provide a reliable alternative to conventional mechanical joining techniques, such as rivets, bolts, and screws, specifically for joining dissimilar structures [5,6]. Nevertheless, during the manufacturing process of bonded joints, different defect scenarios, like adhesive flaws, cohesive flaws, and gross defects such as disbonds, delaminations, foreign inclusions, and porosity have a significant impact on the bonding quality of joints [7,8]. The potential of bonded joints to provide waterproof and lightweight constructions that minimize the risk of corrosion is a major factor driving their rapid use across industries such as aerospace, automobile, electronic, and construction sectors. Defects in adhesive joints during manufacturing and structural damage are often invisible to the human eye or through visual inspection. Therefore, experts have established non-destructive testing techniques to detect and assess these defects without jeopardizing the structural integrity. When it comes to the implementation of bonded joints in critical applications, it is imperative that any discontinuities in these joints be strictly avoided. This is because

[1]Prof. K. Baršauskas Ultrasound Research Institute, Kaunas University of Technology, Kaunas, Lithuania
[2]Department of Electronics Engineering, Kaunas University of Technology, Kaunas, Lithuania
gawher.bhat@ktu.edu, elena.jasiuniene@ktu.lt

these imperfections have the potential to affect human life, environmental safety and economic performance [9,10].

A number of studies on the implementation of different non-destructive testing techniques for the evaluation of bonding quality in adhesive bonded joints have been conducted. Ultrasonic testing is especially valuable for detecting and locating internal defects and assessing the integrity of adhesively bonded joints. In various industries, the probability of detection (POD) is a common way to evaluate the reliability of nondestructive testing (NDT) methods [11]. The reliability of nondestructive testing is influenced by several parameters, including defect morphology, equipment variability, and operator influence. This also contributes to an increase in the number of tests that are conducted for correct POD curve estimation. To overcome these constraints, numerical-simulation-based models can be incorporated into the POD assessment process, substantially minimizing the necessity for huge experimental datasets. Model-Assisted probability of detection (MAPOD) offers cost-effective analysis by simplifying specimens, reducing dimensions, and improving result generalization [12].

Yilmaz et al. [12] conducted the study on Model-Assisted probability of detection (MAPOD) to assess different bonding quality in adhesive joints. Their study particularly focused on how the influence of multiple signal response features impacts the probability of detection and highlighted the significance of proper gate selection and ultrasound signal amplitude in improving the POD of debonding. Carboni and Cantini [13] utilized MAPOD in ultrasonic testing of defects in railway axles to demonstrate the practical usefulness of this method. It was observed that the model-assisted probability of detection could replicate the ultrasonic investigation effectively, thereby enabling the inspection of defect detectability in different scenarios. Rentala et al. [14] in their work on the identification of flat-bottom holes (FBH) employing ultrasonic non-destructive testing, focused on the challenges arising while calibrating models, variability and validation associated with developing MAPOD curves.

In the context of POD analysis, two principal models are commonly used: one based on binary detection (hit/miss) and the other on continuous signal response (signal amplitude or feature value) [15]. This work emphasizes the continuous response POD model, as simulation-based data provides detailed and quantitative signal information, which is better leveraged through the signal response (a v/s â) approach. The findings from the study extend beyond the standard use of maximum amplitude calculation based on CIVA's inbuilt capabilities and contribute to the implementation of different ultrasonic features by integrating the Python based script derived for different interface reflections from features like peak-to-peak amplitude, absolute energy, mean value of amplitude in the frequency domain and absolute time of flight difference.

## 2. Materials & Methodology

The aluminum-epoxy single lap joints used in this study were fabricated at COTESA GmBH, Germany. As illustrated in figure 1, each aluminum plate measured 280×215×1.6 mm. The bonding of the aluminum sheets was achieved using a 0.16 mm thick 3M scotch-Weld AF 163-K red structural epoxy adhesive film. The assembled lap joint had a bonding width of 25 mm. Prior to the adhesive application, the aluminum surface underwent surface preparation to ensure the optimal adhesion and subsequently, the epoxy film was precisely positioned on the adherend to form the adhesive bond. The material properties of the investigation are presented in table I below.

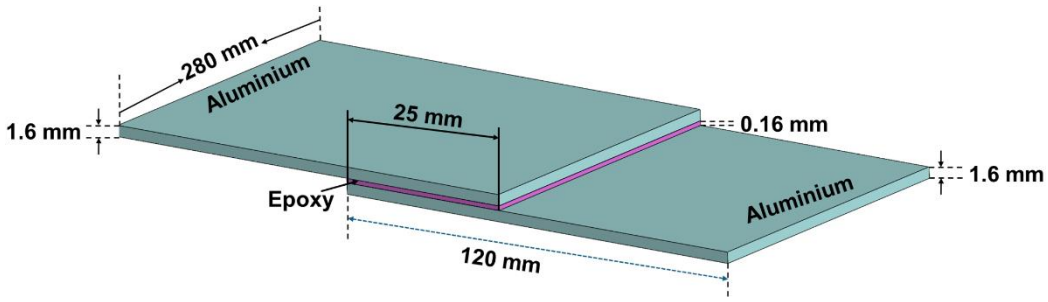


***Figure 1.*** Schematic of the aluminum-epoxy bonded joint

***Table I.*** Material Properties

| **Material Properties** | **Materials** | | | |
|---|---|---|---|---|
| | **Aluminium 2024-T3** | **Epoxy (3M Scotch-Weld AF163-2K)** | **Water** | **Units** |
| Density | 2780 | 1150 | 998 | (kg/m³) |
| Longitudinal velocity | 6320 | 2500 | 1496 | (m/s) |

## 2.1. Methodology

### *2.1.1. Ultrasonic Inspection*

The inspection simulations for the bonded joints were performed using ultrasonic pulse-echo immersion testing to analyze the signal behavior and propagation through the lap joint. All simulations were performed using the CIVA software package, developed by the French atomic Energy Commission (CEA), which allows the realistic modelling of the ultrasonic inspection setups. The results obtained from the simulation on the multi-layer specimen demonstrated the interaction of the ultrasonic signal with internal features, including interfaces and defects. The amplitude and time of the reflected signals were evaluated by examining both A-scan and B-scans, thereby enabling comparison across different defect scenarios. For this investigation, the smallest defect selected had dimensions of 5×5 mm, allowing for the evaluation of the system's sensitivity to small defect detection. Ultrasonic immersion simulation was conducted using a 15 MHz focused transducer with a focal distance of 48 mm in water and a probe diameter of 9.25 mm. To ensure optimal focus on the adhesive interface—where potential flaws are likely to occur, the distance between the transducer and the surface of the bonded joint was calculated using equation 1.

$$W_{path} = f - m_{\delta}\left(\frac{\upsilon_m}{\upsilon_w}\right) \tag{1}$$

Where, $f$ represents focal distance of the probe, $m_{\delta}$ is the material depth, $v_m$ denotes the ultrasonic velocity in the material, and $v_w$ is the water velocity. The complete inspection set-up demonstrating the transducer placement and the material configuration is shown in figure 2.

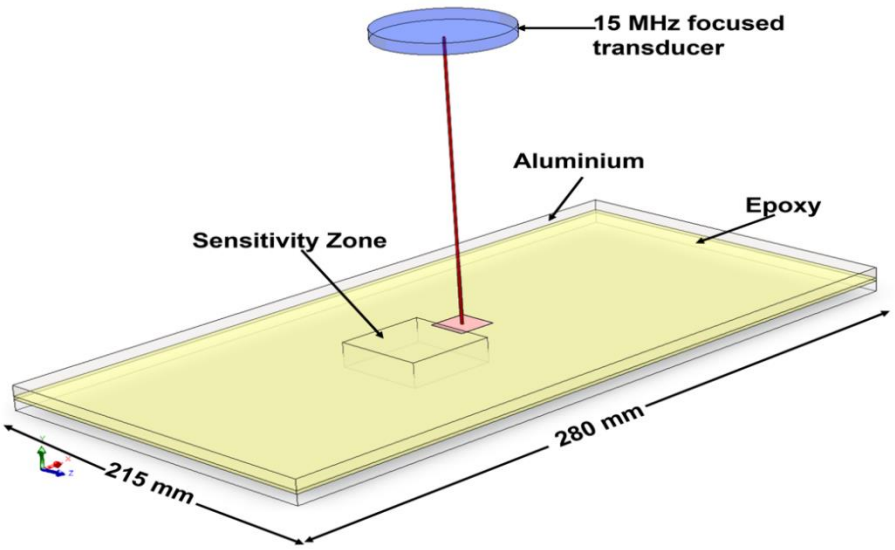


***Figure 2.*** Ultrasonic immersion inspection setup

*2.1.2. Sensitivity Analysis*

*Determination of Influential Parameters*

To achieve the objective of improving defect detection in different ultrasonic features, a sensitivity analysis was carried out using the semi-analytical finite element modelling. The main goal was to identify the key parameters that significantly affect the ability to detect disbonds using the chosen ultrasonic immersion testing technique. Different ultrasonic features which were integrated utilizing the Python based script derived for different interface reflections include features like peak-to-peak amplitude at 2$^{nd}$ reflection, absolute energy at 2$^{nd}$ reflection, and absolute time of flight difference between the 2$^{nd}$ and 3$^{rd}$ interface reflection.

The analysis was performed in two stages: calibration and meta-model computation. In the calibration stage, the system was tuned to determine a reference signal amplitude, specifically, the highest amplitude reflected from the known defective interface. This reference amplitude was then used as a baseline in the meta-model computation stage, where the effects of various parameters were analyzed. The purpose of this sensitivity analysis was to find out which factors most influence the disbond detectability in multi-layered adhesive bonded joints. The uncertain and characteristic parameters considered in this investigation are given in table II.

***Table II.*** Variation range of uncertain parameters

| Parameters | Min Value | Max value | Mean Value | Standard deviation | Units |
|---|---|---|---|---|---|
| Flaw length | 0.01 | 5 | - | 1.44 | mm |
| Aluminium thickness | 1.55 | 1.6 | 1.57 | 0.014 | mm |
| Epoxy Thickness | 0.12 | 0.16 | 0.14 | 0.011 | mm |
| Ultrasound velocity in aluminum | 6340 | 6420 | 6380 | 23.09 | m/s |
| Incidence angle | -3 | 0 | -1.5 | 0.87 | deg |
| Offset of transducer (X axis) | 135 | 145 | 140 | 2.89 | mm |

| | | | | | |
|---|---|---|---|---|---|
| Water path | 43 | 50 | 46.5 | 2.02 | mm |
| Ligament | 1.6 | 1.76 | 1.68 | 0.046 | mm |

The flaw length was chosen as the characteristic parameter, and the flaw height was defined as equal to the flaw length. For the ligament, the flaw depth was estimated using the formulae to make sure that the defect always stays within the epoxy layer.

$$Z_{ligament} = Al_{thickness2nd} + Ep_{thickness} \times (X) \quad (2)$$

Where, $Z_{ligament}$ is the flaw depth, $Al_{thickness2nd}$ is the aluminum plate thickness, and $Ep_{thickness}$ is the epoxy thickness and $X$ is a scaling factor defined for the study varying from [0 to 1].

### *2.1.3. Signal Response Analysis (POD estimation)*

For the computation of the Signal Response POD curve, 16 characteristic values were defined across 5 different samples. The detection threshold was selected based on the ultrasonic simulation results. Especially, the maximum amplitude reflected from the defect-free interface was manually identified to serve as a baseline and subsequently threshold was set at -6 dB, representing the highest background noise level observed in the pristine state. To ensure the reliability of the results, both noise and saturation thresholds were carefully adjusted. These adjustments were made to satisfy the Berens model validity requirements, ensuring that the assumptions of normal distribution and constant variance were met throughout the dataset. A confidence level of 95% was used for the POD analysis, providing a statistically strong estimate of detection capability.

## 3. Results and Discussions

### 3.1.Sensitivity analysis

To build a reliable model, a total of 1000 simulation cases were carried out. These simulations helped capture how different conditions affect the inspection results. A parallel plot in peak-to-peak amplitude at 2nd reflection showing all the simulated cases used to build the model is presented in figure 3. The reliability of the model was analyzed from the actual simulations (called "true" values) which were compared with the model's predicted values using regression and error distribution graphs. The comparison showed that the model is highly reliable and around 86% of the cases had a very small error of 0.02%, which confirms the model's consistency and accuracy.

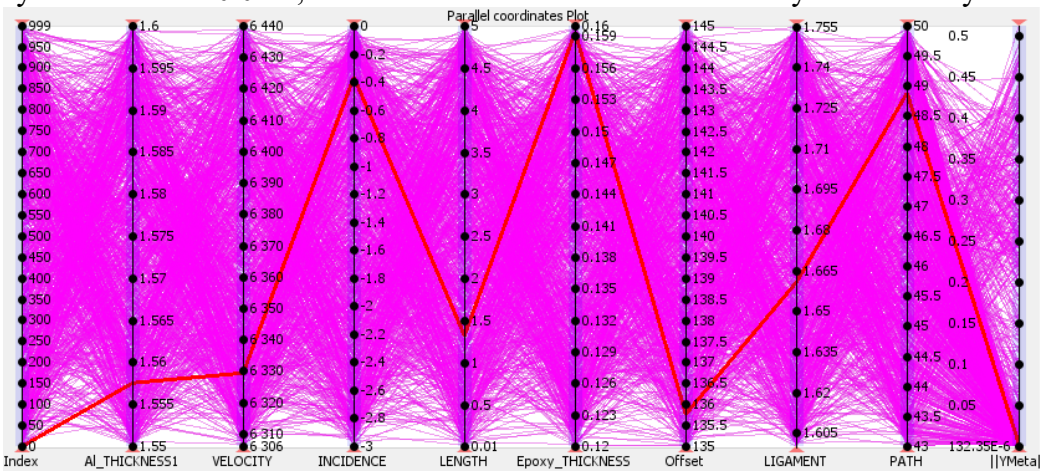


***Figure 3.*** Parallel plot of simulation

Table III and IV shows how sensitive the inspection simulation results are to different uncertain parameters in the ultrasonic features of brass inclusion and delamination sample. The inspection simulation results of sensitivity for both the brass inclusion and delamination are further visualized in the sensitivity diagram illustrated in figure 4 and 5 respectively.

***Table III.*** Sensitivity analysis of uncertain parameters in ultrasonic brass inclusion

| **Parameters** | **Sensitivity, %age** | | |
|---|---|---|---|
| | **Peak-to-peak amplitude at 2nd reflection** | **Absolute energy at 2nd reflection** | **Absolute time-of-flight difference between 2nd and 3rd reflection** |
| Flaw length | 22 | 20 | 15 |
| Aluminium thickness | 8 | 9 | 9 |
| Epoxy Thickness | 9 | 10 | 10 |
| Ultrasound velocity in aluminum | 9 | 9 | 9 |
| Incidence angle | 11 | 12 | 10 |
| Transducer offset | 19 | 13 | 22 |
| Water path | 8 | 7 | 11 |
| Ligament | 15 | 18 | 12 |

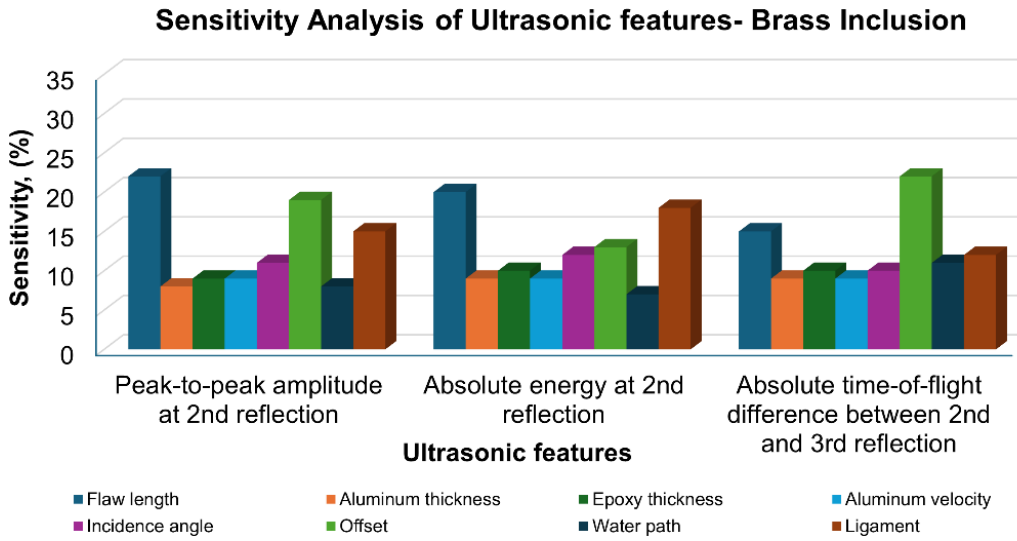


***Figure 4.*** Sensitivity analysis of ultrasonic features in brass inclusion

From the sensitivity analysis diagram of different extracted features of ultrasonic simulation, it was observed that the flaw length has a higher influence on the overall sensitivity. The flaw length in peak-to-peak amplitude at 2nd reflection has a sensitivity of 22% while as for the absolute time-of-flight difference, a 22% sensitivity was observed for the transducer offset. This implies that the flaw size directly influences the probability of damage detection, while as the highest sensitivity in the offset signifies the slightest change of offset position can have a major impact on the overall defect detection reliability.

***Table IV.*** Sensitivity analysis of uncertain parameters in ultrasonic delamination

| **Parameters** | **Sensitivity, %age** | | |
|---|---|---|---|
| | **Peak-to-peak amplitude at 2nd reflection** | **Absolute energy at 2nd reflection** | **Absolute time-of-flight difference between 2nd and 3rd reflection** |
| Flaw length | 29 | 27 | 31 |
| Aluminium thickness | 6 | 7 | 5 |
| Epoxy Thickness | 6 | 5 | 6 |
| Ultrasound velocity in aluminum | 4 | 5 | 4 |
| Incidence angle | 8 | 16 | 9 |
| Transducer offset | 35 | 26 | 33 |
| Water path | 6 | 6 | 6 |
| Ligament | 6 | 8 | 7 |

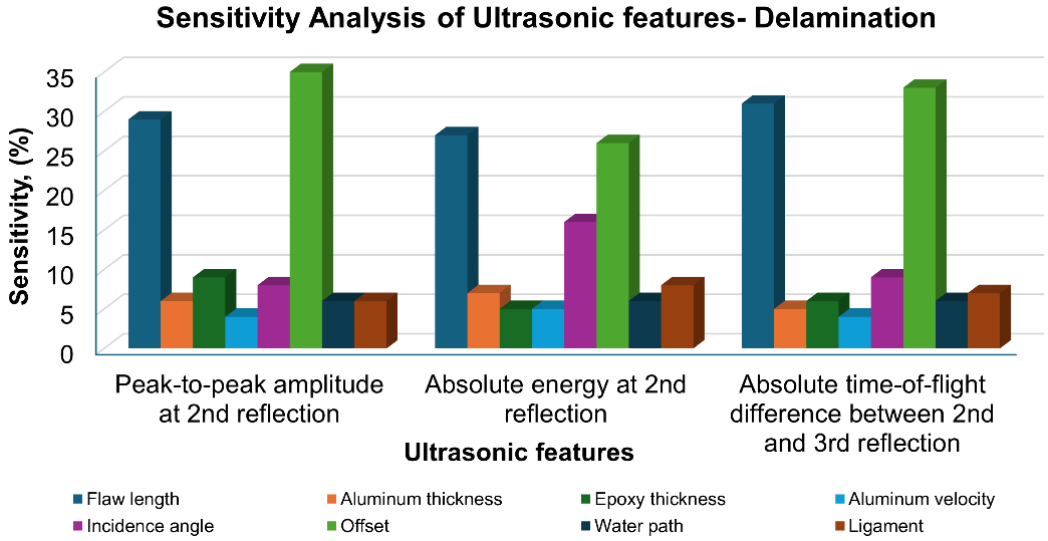


***Figure 5.*** Sensitivity analysis of ultrasonic features in delamination

In case of the delamination sample, it was found that the offset of the transducer along X-axis and the defect size have a major impact on the overall sensitivity. The flaw length in peak-to-peak amplitude at 2nd reflection has a sensitivity of 29% while as for the transducer offset 35% in peak-to-peak amplitude and 33% for the absolute time-of-flight difference was observed. The highest sensitivity in the offset signifies the change in the offset position of the probe can have a major impact on the overall defect detection reliability.

### 3.2. MAPOD curves

The Signal Response POD (Probability of Detection) curve shown in Figure 6 helps evaluate how reliably defects can be found. Based on the results, in 90% of inspections, no defect was detected on the component surface—even when using a 95% confidence level for the standard inbuilt maximum amplitude feature (fig 6 a, b). A consistent POD curve should ideally reach 100% detection probability for larger flaws, but in this case, it falls short. For example, a defect that is 5 mm in size has about 70.12 % chance of being detected (fig 6a). This detection rate is quite low and falls well below the standards typically required in high-safety fields like aerospace. The custom developed features

from the ultrasonic data performed better with satisfying the criteria of 90% probability and reached 95% confidence level for all the cases in both the brass inclusion and delamination sample. The best performing features from both the inspection are presented in figure (6 c, d) in comparison with the standard maximum amplitude (Amax) case.

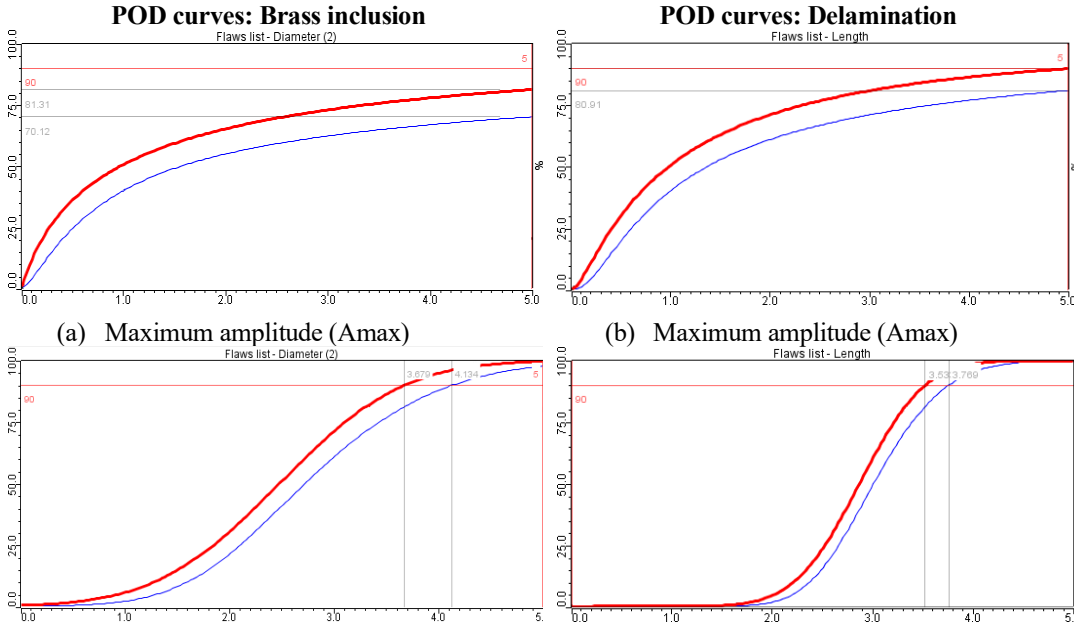


(a) Maximum amplitude (Amax)

(b) Maximum amplitude (Amax)

(c) Absolute time of flight difference between 2nd and 3rd interface reflection

(d) Peak-to-peak amplitude at 2nd interface reflection

***Figure 6.*** POD curves for brass inclusion and delamination defect type for standard Amax and extracted ultrasonic features

For the brass inclusion, a defect size of 3.67 mm was detected with a probability of 90% in the absolute time of flight difference between 2nd and 3rd interface reflection. While as for the delamination, a defect size measuring 3.53 mm was detected in the peak-to-peak amplitude at 2nd interface reflection with a probability of 90%.

## 4. Conclusion

The POD (Probability of Detection) curves were evaluated using signal response analysis, based on a predictive model and a detection threshold set at the highest noise level—taken from the reflection at the defect-free bond line. The results clearly showed that using the standard ultrasonic inspection alone, it is not possible to reliably detect disbonds within the adhesive layer of joints. The detection success rate was only about 70.12%, which is far too low to meet the standards required for dependable flaw detection, especially in critical applications.

The major findings of this study highlight the significance of feature selection like peak-to-peak amplitude at 2nd interface reflection, energy of signal at 2nd reflection, and absolute time-of-flight difference between 2nd and 3rd interface reflection in ultrasonic non-destructive testing thereby demonstrating the capability of improving defect detection in adhesively bonded joints. The results validate the efficacy of the selected method by ensuring its reliability in detecting flaws with improved accuracy.


## ACKNOWLEDGMENT

This research was funded by COST Action CA21155 – HISTRATE (Advanced Composites under High STRAin raTES loading: a route to certification-by-analysis) with fundings from the COST Association (European Cooperation in Science and Technology) funded by the European Union.

## REFERENCES

1. Adams, R. D., Comyn, J., & Wake, W. C. (1997). Structural adhesive joints in engineering. Springer Science & Business Media.
2. SatyanarayanaGupta, M., & Veeranjaneyulu, K. (2017). Fabrication and anayisis of adhesive joints used in aircraft structures. Materials Today: Proceedings, 4(8), 8279-8286.
3. Romano, M. G., Guida, M., Marulo, F., Giugliano Auricchio, M., & Russo, S. (2020). Characterization of adhesives bonding in aircraft structures. Materials, 13(21), 4816.
4. Hart-Smith, J. (2021). Aerospace industry applications of adhesive bonding. In Adhesive bonding (pp. 763-800). Woodhead Publishing.
5. Tan, B., Hu, Y., Yuan, B., Hu, X., & Huang, Z. (2021). Optimizing adhesive bonding between CFRP and Al alloy substrate through resin pre-coating by filling micro-cavities from sandblasting. International Journal of Adhesion and Adhesives, 110, 102952.
6. Zimmermann, N., & Wang, P. H. (2020). A review of failure modes and fracture analysis of aircraft composite materials. Engineering failure analysis, 115, 104692.
7. Bhat, G. A., Smagulova, D., & Jasiūnienė, E. (2025). Improved Defect Sizing in Adhesive Joints Through Feature-Based Data Fusion. Journal of Nondestructive Evaluation, 44(1), 14.
8. Smagulova, D., Mazeika, L., & Jasiuniene, E. (2021). Novel processing algorithm to improve detectability of disbonds in adhesive dissimilar material joints. Sensors, 21(9), 3048.
9. Wei, Y., Jin, X., Luo, Q., Li, Q., & Sun, G. (2024). Adhesively bonded joints–a review on design, manufacturing, experiments, modeling and challenges. Composites Part B: Engineering, 276, 111225.
10. Meshkizadeh, P., & Farahani, M. (2024). Progress in nondestructive evaluation and condition monitoring of adhesive joints. Progress in Adhesion and Adhesives, 8, 361-404.
11. Tai, J. L., Hameed Sultan, M. T., Shahar, F. S., Yidris, N., Basri, A. A., & Md Shah, A. U. (2024). Exploring Probability of Detection (POD) Analysis in Nondestructive Testing: A Comprehensive Review and Potential Applications in Phased Array Ultrasonic Corrosion Mapping. Pertanika Journal of Science & Technology, 32(5).
12. Yilmaz, B., Smagulova, D., & Jasiuniene, E. (2022). Model-assisted reliability assessment for adhesive bonding quality evaluation with ultrasonic NDT. NDT & E International, 126, 102596.
13. Carboni, M., & Cantini, S. (2012, April). A model assisted probability of detection approach for ultrasonic inspection of railway axles. In 18th world conference on nondestructive testing (pp. 16-20).
14. Rentala, V. K., Mylavarapu, P., & Gautam, J. P. (2018). Issues in estimating probability of detection of NDT techniques–A model assisted approach. *Ultrasonics*, *87*, 59-70.
15. Berens, A. P. (1981). Evaluation of NDE reliability characterization. Report No. AFWAL-TR-81-4160.